Diffraction from non-Gaussian rough surfaces

Y.-P. Zhao, G.-C. Wang, and T.-M. Lu

Department of Physics, Applied Physics, and Astronomy and Center for Integrated Electronics and Electronics Manufacturing,
Rensselaer Polytechnic Institute, Troy, New York 12180-3590

Most diffraction theories for random rough surfaces are based on the assumption of a Gaussian height distribution. In this paper, a diffraction theory for non-Gaussian rough surfaces is developed and the relationship between the roughness parameters and the diffraction characteristics is explored. It is shown that a non-Gaussian rough surface can dramatically alter the diffraction for $(k_\perp w)^2 \gg 1$, where $k_\perp$ is the momentum transfer perpendicular to the surface and w is the interface width. However, for $(k_\perp w)^2 \ll 1$, it is possible to determine all the roughness parameters including the interface width, lateral correlation length, and the roughness exponent without specifying the surface height distribution. [S0163-1829(97)06116-X]

I. INTRODUCTION

Recently, there has been intense interest in the study of statistically rough surfaces that are generated in processes such as the growth and etching of thin films.[1–3] A fundamental understanding of the microscopic aspects of the dynamics of interface evolution is of prime interest not only for thin-film growth and material science, but also for numerous technological applications. A hypothesis of dynamic scaling has been used to describe the interface evolution. Under a far-from-equilibrium condition, the morphology of a growing interface is proposed to have a self-affine form. The interface width w, which describes the root-mean-square surface height fluctuation, is scaled with the finite size L of the system and time t as[1–3]

$$w(L,t) = L^\alpha f\left(\frac{t}{L^z}\right), \quad (1)$$

where $z = \alpha/\beta$. The scaling function $f(x)$ is given by

$$f(x) \approx \begin{cases} x^\beta & \text{for } x \ll 1 \\ \text{const} & \text{for } x \gg 1 \end{cases}. \quad (2)$$

For $L^z \gg t$, the interface width grows with time in the form of a power law $w \sim t^\beta$, while for $L^z \ll t$, $w \sim L^\alpha$, showing that the interface morphology has a stationary self-affine form. The exponent β describes the growth rate of the interface width. The roughness exponent α (where $0 \leq \alpha \leq 1$) is a measure of the local surface roughness. The hypothesis of dynamic scaling also leads to an equal-time height-height correlation of the form[1–3]

$$H(\mathbf{r},t) = \langle [h(\mathbf{r},t) - h(0,t)]^2 \rangle = 2[w(t)]^2 g\left(\frac{r}{\xi(t)}\right), \quad (3)$$

where $\mathbf{r}$ is the spatial vector on a surface, $h(\mathbf{r},t)$ is the surface height at position $\mathbf{r}$ and time t, $g(x) = x^{2\alpha}$ for $x \ll 1$, and $g(x) = 1$ for $x \gg 1$. Here ξ is called the lateral correlation length, denoting the correlation parallel to the surface. Within the dynamic scaling approach, different growth models, such as random deposition,[4–6] the Eden model,[7–9] ballistic deposition,[10,11] the Kardar-Parisi-Zhang (KPZ) model,[12]

the restricted solid-on-solid model,[13] and the Molecular-beam-epitaxy (MBE) growth model,[14–17] would give different values for the exponents α and β.

Experimentally, the most direct method to obtain surface roughness parameters quantitatively is to measure the height-height correlation of the surface using real-space imaging techniques, such as scanning tunneling microscopy, atomic-force microscopy, secondary electron microscopy, transmission electron microscopy, and optical imaging techniques. However, measurement by these methods often interrupts the growth process, which sometimes is not desirable for practical purposes. Diffraction techniques, such as electron diffraction, x-ray diffraction, atom diffraction, and light scattering, provide an alternative way to study the surface morphology quantitatively. An attractive feature of many of these techniques is that they can be used for *in situ*, real-time monitoring of the growth process without interruption.[18] Until now, all the diffraction theories from self-affine random rough surface had been based on the assumption of a Gaussian height distribution of the random surface.[19–21] This assumption can lead to some very simple asymptotic relations between the diffraction profile and the roughness parameters.[19–21] These relations are the basis for rough surface analysis by diffraction.[22] However, in practice, the surface height distribution is not always Gaussian.

In Sec. II of this paper we discuss the existence of a non-Gaussian height distribution in various growth models. In Sec. III, based on a mathematical theorem on the joint distribution of a known marginal distribution function and a known correlation function, we discuss diffraction from various surfaces with different height distributions. A comparison between the Gaussian distribution and other distributions is given. Section IV gives a short conclusion.

II. EXAMPLES OF NON-GAUSSIAN HEIGHT DISTRIBUTIONS IN SURFACE EVOLUTION

Random rough surfaces are often treated as a result of stochastic processes with respect to $\mathbf{r}$. For a stochastic process, it is possible for different processes to have the same correlation function but different height distributions or vice versa. Therefore, in order to determine the properties of a

certain stochastic process, not only should the distribution be given, but also the correlation function, as well as higher-order correlators. Traditionally, for surface growth, more emphasis has been placed on the height-height correlation or the autocorrelation rather than the height distribution. Theoretically, once both the mean and the correlation of the noise term in a linear Langevin equation are given, the height-height correlation function can be determined. A simple example is the Edwards-Wilkison model[4]

$$\frac{\partial h}{\partial t} = \nu \nabla^2 h + \eta(\mathbf{r}, t),\qquad(4)$$

where ν is the surface tension and η is the noise term. Very often $\eta(\mathbf{r}, t)$ is assumed to be a white noise, satisfying the relations

$$\langle \eta(\mathbf{r}, t) \rangle = 0,$$
$$\langle \eta(\mathbf{r}, t) \eta(\mathbf{r}', t') \rangle = 2D\delta(\mathbf{r} - \mathbf{r}')\delta(t - t'),\qquad(5)$$

where D is the fluctuation of the noise. Notice that there is no assumption about the distribution. Equation (4) can be solved through the spatial Fourier transformation and the corresponding height-height correlation function can be obtained

$$H(\mathbf{r}, t) \propto \int_0^{1/b_c} [1 - U(qr)] \frac{1 - e^{-2\nu q^2 t}}{q^{3-d}} \, dq,\qquad(6)$$

where b_c is the short-scale cutoff (within an order of the lattice constant), $U(qr) = J_0(qr)$ for $d = 2$, and $U(qr) = \cos(qr)$ for $d = 1$. Here J_0 stands for the zeroth-order Bessel function. It is obvious that $H(\mathbf{r}, t)$ does not depend on the height distribution.

If we want to know the time evolution of the distribution of $h(\mathbf{r}, t)$, a more detail assumption about the statistical characteristics of $\eta(\mathbf{r}, t)$ should be made. As the nth-order correlation of the noise term $\eta(\mathbf{r}, t)$ is defined, the solution of the Langevin equation would satisfy a certain master equation. A very simple case is to assume that $\eta(\mathbf{r}, t)$ is a Gaussian-Markov process, i.e., $\eta(\mathbf{r}, t)$ not only satisfies Eq. (5), but also meets the following conditions: For odd n,

$$\langle \eta(\mathbf{r}_1, t_1) \eta(\mathbf{r}_2, t_2) \cdots \eta(\mathbf{r}_n, t_n) \rangle = 0;\qquad(7a)$$

for even n,

$$\langle \eta(\mathbf{r}_1, t_1) \eta(\mathbf{r}_2, t_2) \cdots \eta(\mathbf{r}_n, t_n) \rangle$$
$$= \alpha_1 \delta(\mathbf{r}_1 - \mathbf{r}_2) \delta(\mathbf{r}_3 - \mathbf{r}_4) \cdots \delta(\mathbf{r}_{n-1} - \mathbf{r}_n) \delta(t_1 - t_2)$$
$$\times \delta(t_3 - t_4) \cdots \delta(t_{n-1} - t_n) + \alpha_2 \delta(\mathbf{r}_1 - \mathbf{r}_3)$$
$$\times \delta(\mathbf{r}_2 - \mathbf{r}_4) \cdots \delta(t_1 - t_3) \delta(t_2 - t_4) \cdots + \cdots ;\qquad(7b)$$

i.e., the ensemble average of $n = 2m$ product of $\eta(\mathbf{r}_1, t_1)$ is expressed as all the possible linear combinations of $2m$ delta functions. For a Gaussian-Markov process, the corresponding master equation can be reduced to a Fokker-Planck equation. If we denote by $P[h(\mathbf{r}), t]$ the distribution functional of the surface position function $h(\mathbf{r})$, the corresponding Fokker-Planck equation for Eq. (4) is[23]

$$\frac{\partial P[h, t]}{\partial t} = -\nu \int d\mathbf{r} \frac{\delta}{\delta h} [P \nabla^2 h] + D \int d\mathbf{r} \frac{\delta^2}{\delta h^2} P.\quad(8)$$

It has been proved that the solution for Eq. (8) is Gaussian. However, if other statistical properties are satisfied [instead of just Eq. (7)], then the Fokker-Planck equation will not take the form of Eq. (8) and the distribution will not be a Gaussian distribution.

For a nonlinear Langevin equation, even if $\eta(\mathbf{r}, t)$ is a Gaussian-Markov process, the height distribution may not possess the Gaussian form. A famous example is the KPZ model[12]

$$\frac{\partial h}{\partial t} = \nu \nabla^2 h + \frac{\lambda}{2} (\nabla h)^2 + \eta(\mathbf{r}, t),\qquad(9)$$

where λ is proportional to the growth rate. The appearance of the nonlinear term $(\nabla h)^2$ breaks the up/down symmetry, the symmetry of the interface fluctuations with respect to the mean interface height, and the height distribution becomes asymmetric. The Fokker-Planck equation for Eq. (9) is

$$\frac{\partial P[h, t]}{\partial t} = -\int d\mathbf{r} \frac{\delta}{\delta h} \left\{ \left[\nu \nabla^2 h + \frac{\lambda}{2} (\nabla h)^2 \right] P \right\}$$
$$+ D \int d\mathbf{r} \frac{\delta^2}{\delta h^2} P.\qquad(10)$$

The solution for Eq. (10) in $1+1$ dimensions can be written as[23]

$$P(\Delta h) \approx \begin{cases} \exp\left[-\frac{(\Delta h)^2}{L} \right] & \text{for } t \gg L^z \\ \exp\left[-\left(\frac{|\Delta h|}{t^{1/3}} \right)^v \right] & \text{for } t \ll L^z \end{cases}.\qquad(11)$$

Here $\Delta h = h - \langle h \rangle$; for $\Delta h > 0$, $v = \frac{3}{2}$, and for $\Delta h < 0$, $v \approx 2.5$. For evolution over a long time, the surface height reaches the steady-state Gaussian distribution, while over a short time, it is a skewed distribution.

To make it clear, we plot in Fig. 1 our results obtained from the numerical integration of the KPZ equation in $2+1$ dimensions with a system size of 256×256 at the initial stage. The noise term $\eta(\mathbf{r}, t)$ is simulated by a random noise generator with Gaussian distribution. Figure 1(a) shows how the surface height distribution evolved with the number of iterations t. The solid curve represents the best Gaussian fit. Figure 1(b) shows the skewness and kurtosis [defined later in Eq. (36)] versus the number of iterations. For a Gaussian distribution, the skewness is equal to 0.0 and the kurtosis is equal to 3.0, as seen for $t = 0$. However, for $t > 0$, the skewness is greater than 0.0, which shows the asymmetric distribution of the surface height. (For $2+1$ dimensions the height distribution does not approach a steady-state Gaussian distribution.)

Another important example is surface roughness generated by Schwoebel barrier effects during MBE growth, which has been shown to possess a non-Gaussian height distribution.[24] Roughness structures generated as a result of Schwoebel barriers effect are not self-affine and therefore do not possess the dynamic scaling properties described by Eq. (3). Interesting results have been obtained to describe the
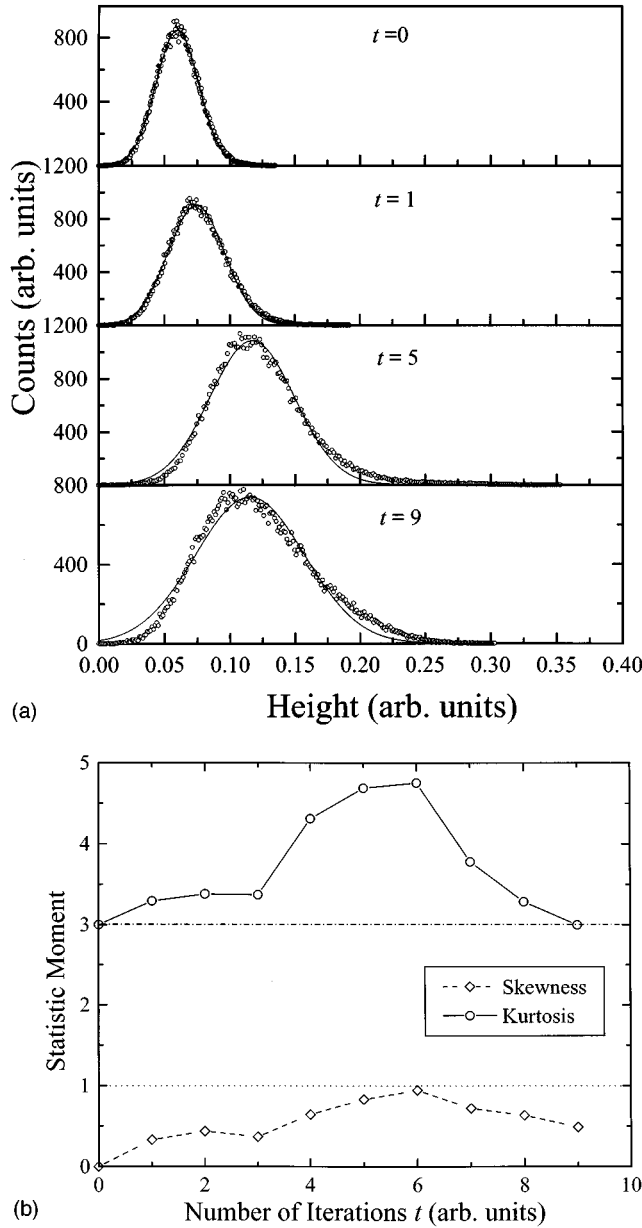
(a)

(b)

FIG. 1. (a) Evolution of surface height distribution as the number of iterations t for the KPZ model in the $(2+1)$-dimensional case: numerical results. (b) Higher-order moment coefficient skewness and kurtosis versus the number of iterations t in the KPZ model in the $(2+1)$-dimensional case.

diffraction characteristics of these Schwoebel-barrier-induced rough surfaces under certain diffraction conditions.[24]

III. DIFFRACTION FROM NON-GAUSSIAN DISTRIBUTED RANDOM ROUGH SURFACE

In general, the diffraction profile can be written as[21]

$$S(\mathbf{k}) = \int d^2 r \ C(k_\perp, r) e^{i\mathbf{k}_\parallel \cdot \mathbf{r}}, \quad (12)$$

where $\mathbf{k}_\parallel$ and $k_\perp$ are momentum transfers parallel and perpendicular to the surface, respectively, and $C(k_\perp, r)$ is called the height difference function, defined as

$$C(k_\perp, r) = \langle e^{ik_\perp[h(\mathbf{r}+\boldsymbol{\rho}) - h(\boldsymbol{\rho})]} \rangle, \quad (13)$$

where $\boldsymbol{\rho}$ is a position vector on the surface. If we denote $h(\mathbf{r}+\boldsymbol{\rho}) - h(\boldsymbol{\rho})$ as z, it is clear that $C(k_\perp, r)$ is the characteristic function of the distribution of z. In order to calculate $C(k_\perp, r)$ and the distribution of z, one needs to know the joint distribution function f^J of $h(\mathbf{r}+\boldsymbol{\rho})$ and $h(\boldsymbol{\rho})$. As discussed above, the direct method to do this is to create the corresponding master or Fokker-Planck equation from the known Langevin equation and then to obtain the height distribution and related joint distribution by solving the equation. However, solving the master or Fokker-Planck equation is not trivial due to the various distributions of noise and nonlinearity. It is even harder to get an analytical solution. A simpler way is to make assumptions about the height distributions. Since we only consider the self-affine surface, the autocorrelation function is already known through Eq. (3). The problem reduces to finding the joint distribution f^J given the height distribution and the correlation function. This problem has been attacked by many people over the past 40 years.[25-27] Beckmann summarizes those results as the following theorem.[27]

Theorem. Let X and Y be two identically distributed random variables with given probability density $f(x)$ and given correlation coefficient $R(r) \geqslant 0$ and let X and Y be independent for $R=0$. If $f(x)$ is proportional to the weighting function of one of the standard classical system of orthogonal polynomials $\{Q_n\}$, then the joint density of X and Y is

$$f^J(x,y;R) = f(x)f(y) \sum_{n=0}^{\infty} \frac{R^n(r)}{h_n^2} Q_n(x) Q_n(y), \quad (14)$$

where

$$\int_a^b f(x) Q_n(x) Q_m(x) dx = h_n^2 \delta_{nm}, \quad (15a)$$

$$R(r) = \frac{\langle xy \rangle - \langle x \rangle \langle y \rangle}{\sqrt{(\langle x^2 \rangle - \langle x \rangle^2)(\langle y^2 \rangle - \langle y \rangle^2)}}. \quad (15b)$$

$R(r)$ is also called the autocorrelation function when x and y are random variables of the same random process. Here we propose another method that starts from the general one-variable Langevin equation and obtained a slightly different expression from Eq. (14). Appendix A shows the detailed deduction. Then Eq. (14) can be modified as

$$f^J(x,y;R) = f(x)f(y) \sum_{n=0}^{\infty} \frac{R(r)^{\lambda_n/\lambda_1}}{h_n^2} Q_n(x) Q_n(y), \quad (16)$$

where λ_n is the eigenvalue of $Q_n(x)$ for the corresponding eigenequation. The only difference between Eqs. (16) and (14) is that the power n of R in Eq. (14) is changed to the eigenvalue of $Q_n(x)$ for the corresponding eigenequation. However, the proof of Eq. (16) is more general than that of Ref. 27.

For the self-affine surface, the height-height correlation function $H(r)$ and the autocorrelation function $R(r)$ are related according to the equation

$$H(r) = 2w^2[1 - R(r)]. \quad (17)$$

TABLE I. Summary of the basic results of different height distributions.

Distribution	Height distribution function $f(x)$	Variance $\langle[x-\langle x\rangle]^2\rangle$	Height difference distribution function $p(z,r)$	Height difference function $C(k_\perp,r)$
Gaussian	$\dfrac{1}{\sqrt{2\pi}w}\exp\left(-\dfrac{x^2}{2w^2}\right)$	w^2	$\dfrac{1}{2w\sqrt{\pi(1-R)}}\exp\left(-\dfrac{z^2}{4w^2(1-R)}\right)$	$\exp[-\tfrac{1}{2}k_\perp^2 H(r)]$
exponential	$\dfrac{1}{w}\exp\left(-\dfrac{x}{w}\right)$	w^2	$\dfrac{1}{2w\sqrt{1-R}}\exp\left(-\dfrac{|z|}{w\sqrt{1-R}}\right)$	$\dfrac{1}{1+\tfrac{1}{2}k_\perp^2 H(r)}$
Γ	$\dfrac{1}{\Gamma(\kappa+1)\sigma^{\kappa+1}}x^\kappa e^{-x/\sigma}$	$(\kappa+1)\sigma^2$	$\dfrac{1}{\Gamma(\kappa+1)\sigma\sqrt{\pi}(1-R)^{\kappa+1}}\left(\dfrac{z\sqrt{1-R}}{2\sigma}\right)^{\kappa+1/2}$ $\times K_{\kappa+1/2}\left(\dfrac{z}{\sigma\sqrt{1-R}}\right)$	$\dfrac{1}{\left(1+\dfrac{k_\perp^2 H(r)}{2(\kappa+1)}\right)^{\kappa+1}}$
uniform	$\dfrac{1}{2a}$	$\dfrac{a^2}{3}$	$\dfrac{1}{4a^2}\sum_{n=0}^{\infty}(2n+1)R^{n(n+1)/2}$ $\times\int_{x_1}^{x_2}P_n\left(\dfrac{y+z}{a}\right)P_n\left(\dfrac{y}{a}\right)dy$	$\dfrac{\pi}{2k_\perp a}\sum_{n=0}^{\infty}(2n+1)$ $\times R^{n(n+1)/2}J_{n+1/2}^2(k_\perp a)$
Rayleigh	$\dfrac{x}{\sigma^2}\exp\left(-\dfrac{x^2}{2\sigma^2}\right)$	$\dfrac{4-\pi}{2}\sigma^2$	$\int_0^\infty\dfrac{y(y+z)}{\sigma^4(1-R)}\exp\left(-\dfrac{y^2+(z+y)^2}{2\sigma^2(1-R)}\right)$ $\times I_0\left(\dfrac{y(y+z)\sqrt{R}}{\sigma^2(1-R)}\right)dy$	$\sum_{n=0}^{\infty}\dfrac{\pi k_\perp\sigma^2}{2}\left[\left(-\dfrac{1}{2}\right)_n\right]^2$ $R^n\,{}_2F_2^2\left(\dfrac{3}{2},\dfrac{3}{2},\dfrac{3}{2},\dfrac{3}{2}-n;-\dfrac{k_\perp^2\sigma^2}{2}\right)$

It is clear that for $r\to0$, $R\to1$, and for $r\to\infty$, $R\to0$, i.e., R satisfies the condition stated in the theorem. If we denote x as $h(\mathbf{r}+\boldsymbol{\rho})$, y as $h(\boldsymbol{\rho})$, and $f(x)$ as the weighting function of a system of classical polynomials Q_n, then the joint distribution f^J is given by Eq. (16). The distribution of $z(r)$ $(=x-y)$ (height difference distribution) is expressed as

$$p(z,r)=\int f^J(y+z,y;R(r))dy. \quad (18)$$

With this definition, $C(k_\perp,r)$ can be written as

$$C(k_\perp,r)=\int p(z,r)e^{ik_\perp z}dz \quad (19)$$

or

$$C(k_\perp,r)=\int\int f^J(x,y;R(r))e^{ik_\perp(x-y)}dx\,dy$$
$$=\sum_{n=0}^{\infty}\frac{R(r)^{\lambda_n/\lambda_1}}{h_n^2}\left|\int f(x)Q_n(x)e^{ik_\perp x}dx\right|^2. \quad (20)$$

The derivation of $p(z,r)$ and $C(k_\perp,r)$ for various continuous and discrete distributions is given in Appendix B and the results are summarized in Table I.

A. The height difference distribution $p(z,r)$ and height difference function $C(k_\perp,r)$

Table I shows that, for the Gaussian height distribution, the height difference $z(r)$ also obeys a Gaussian distribution

with the variance associated with the autocorrelation coefficient R. For exponential height distribution $(\Gamma(0,x))$, the height difference $z(r)$ is also an exponential distribution with $z(r)$ ranging from $-\infty$ to $+\infty$, while x ranges from 0 to $+\infty$. The height difference distribution for a Γ height distribution is a K distribution [see Eq. (B24) in Appendix B]. As seen from Table I, all the variances for the height difference distribution are modified by the autocorrelation coefficient R. We plot in Figs. 2 and 3 various height distributions and the corresponding height difference distributions with the same standard deviation and $R=0.5$. The Gaussian distribution is symmetric with respect to its mean and has nonzero even central moments and no odd central moments. The Γ distributions are not symmetric with respect to their mean, especially for $\kappa=0$, which is the same as the exponential distribution. They are the skewed distributions with nonzero odd central moments. However, the height difference distributions are symmetric with the means equal to zero. The greatest difference between the Gaussian distribution and Γ distribution with respect to their height difference distributions is that $p(z,r)$ for the Γ distribution has higher probability around $z=0$, narrower distribution width, and a longer tail than that for the Gaussian distribution. As we shall see later, this difference will have a more dramatic effect in the diffraction profiles at large $k_\perp$.

The height difference function $C(k_\perp,r)$ also takes different forms for different height distributions as seen in Table I. $C(k_\perp,r)$ is a function of $H(r)$, the height-height correlation function. Denoting $\Omega=(k_\perp w)^2$, we have

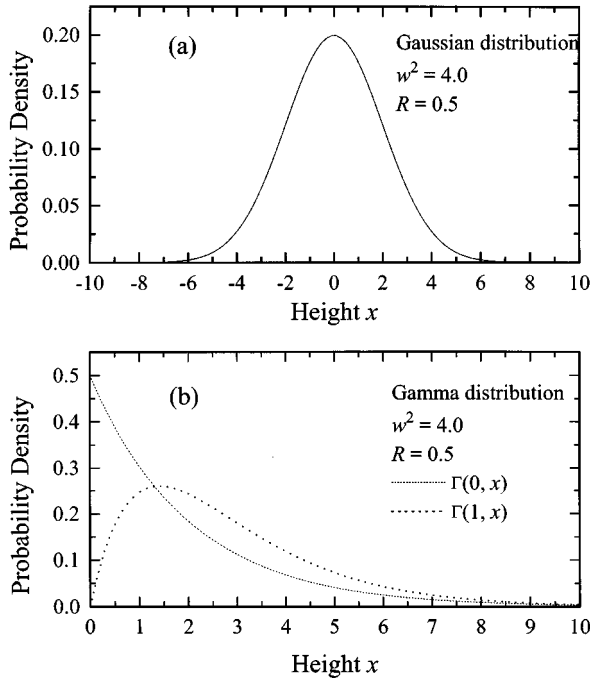FIG. 2. Surface height distribution $f(x)$ for different statistical models: Gaussian and Γ distributions.

$$C(k_\perp, r) = F(\Omega g(r/\xi)), \qquad (21)$$

where $g(x)$ is the scaling function, which we would like to take the form suggested by Sinha, Sirota, and Garoff,[19]

$$g(x) = 1 - e^{-x^{2\alpha}}. \qquad (22)$$

The plot of $C(k_\perp, r)$ for $\Omega \ll 1$ and $\Omega \gg 1$ for different height distributions is shown in Figs. 4(a) and 4(b). Here we assume $\alpha = 0.75$ and $\xi = 5.0$. For $\Omega \ll 1$ the differences in $C(k_\perp, r)$ for various distributions are very small, while for $\Omega \gg 1$ the differences are more obvious. In fact, from Table I for $\Omega \ll 1$ all the height difference functions $C(k_\perp, r)$ can be approximated by
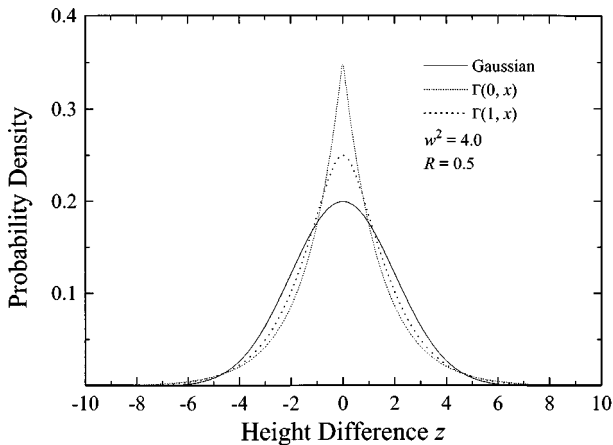
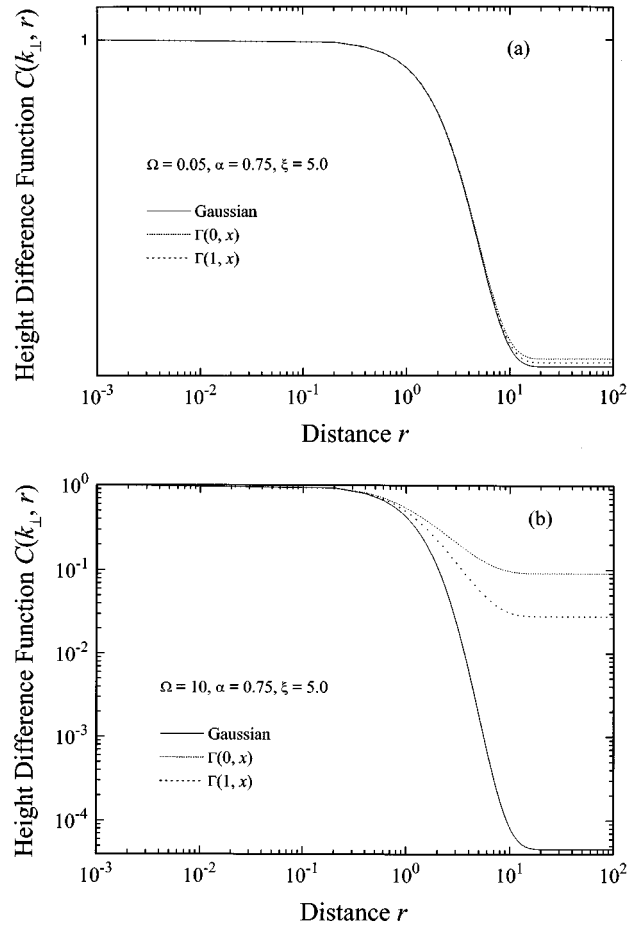FIG. 3. Height difference distributions $p(z, r)$ for different surface height distributions.

FIG. 4. Height difference function $C(k_\perp, r)$ for different height distributions: (a) $\Omega \ll 1$ and (b) $\Omega \gg 1$.

$$C(k_\perp, r) \approx 1 - \frac{1}{2} k_\perp^2 H(r). \qquad (23)$$

As long as $H(r)$ is the same, $C(k_\perp, r)$ will be the same no matter what the height distribution is. Actually, Eq. (23) can be derived directly from the definition of $C(k_\perp, r)$ in Eq. (13). This is a very useful result as we shall discuss later. For $\Omega \gg 1$ higher-order moments in Eq. (13) will take effect. These moments depend on the height distribution as seen from Eq. (20). For a Gaussian height distribution $C(k_\perp, r)$ decreases very fast as a function of r, while for a Γ height distribution the decrease is slower, as shown in Fig. 5. The abrupt decrease of $C(k_\perp, r)$ for the Gaussian height distribution gives more higher-frequency terms in the Fourier transform and the diffuse profile would be much broader than that obtained from the Γ distributions, as to be seen later in Fig. 12.

For the discrete surface such as steps, we compare the Gaussian height distribution and Poisson height distribution. As shown in Fig. 6, the Poisson distribution is also a skewed distribution with nonzero odd moments. As the standard deviation a increases, the distribution becomes more symmetric. The height difference distribution for the Poisson height
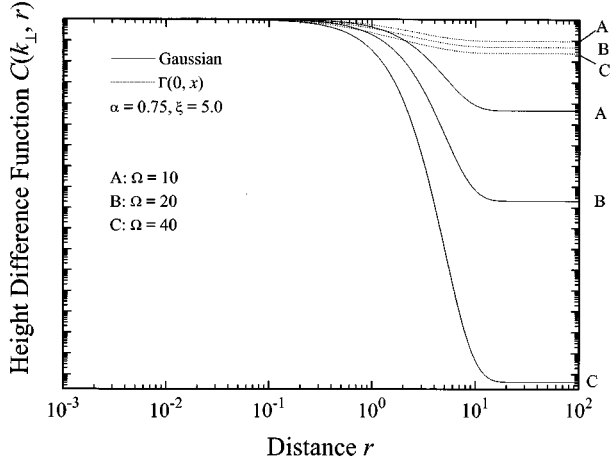
FIG. 5. Change of the height difference function $C(k_\perp,r)$ with respect to different Ω ($=k_\perp^2 w^2$) values.

distribution is the modified Bessel function with respect to the order of n. In Fig. 7 we plot the height difference distribution $p(z,r)$ for both Gaussian and Poisson distributions with a variance of 4.0. Like the Γ distribution for the continuous surface, $p(z,r)$ for Poisson distribution has a longer tail than that for the Gaussian distribution. As discussed in Ref. 21, the discrete lattice effect has a significant consequence on the height difference function. In the continuous surface case, Eq. (21) shows that the height difference function $C(k_\perp,r)$ is a function of Ω, in which $k_\perp$ and w play a similar role in $C(k_\perp,r)$. But for the discrete surface $k_\perp$ and w do not play the same role in $C(k_\perp,r)$. For the Poisson distribution, in Appendix A we show that

$$C(k_\perp,r) = e^{-H(r)(1-\cos\Phi)}, \qquad (24)$$

where phase $\Phi = k_\perp c$ and c is the lattice constant. For the Gaussian distribution we have[3]

$$C(k_\perp,r) = \frac{\displaystyle\sum_{m=-\infty}^{+\infty} e^{-(1/2)H(r)(\Phi-2\pi m)^2}}{\displaystyle\sum_{m=-\infty}^{+\infty} e^{-(1/2)H(r)(2\pi m)^2}}. \qquad (25)$$
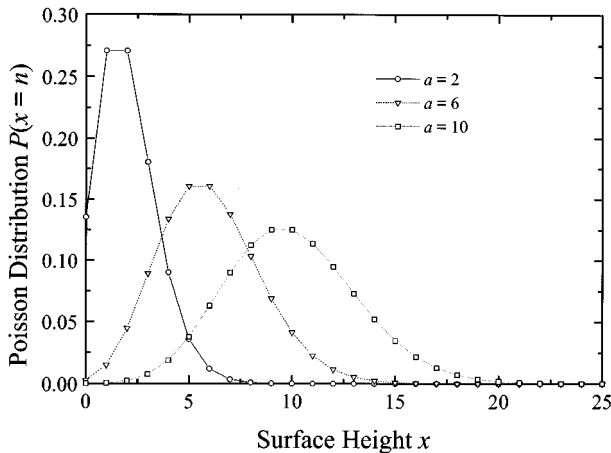

FIG. 6. Poisson distribution with various variances a. Here the surface height n is in the units of the lattice constant.
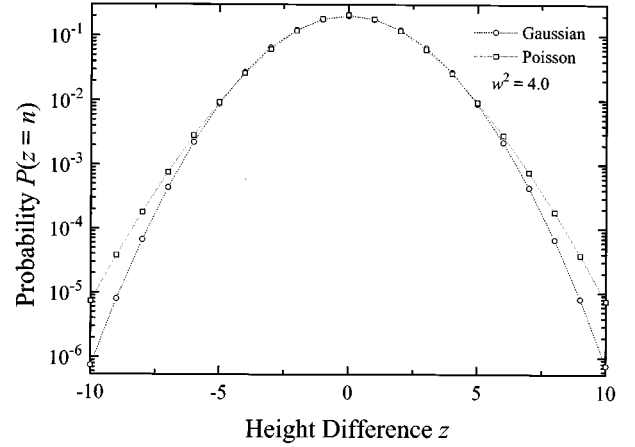

FIG. 7. Height difference distribution $p(z,r)$ in the discrete lattice with different height distributions.

Both Eqs. (24) and (25) indicate that $C(k_\perp,r)$ is a periodic function of $k_\perp$ and it decays exponentially with w^2, which is imbedded in $H(r)$. The periodic oscillatory behavior of $C(k_\perp,r)$ for both Gaussian and Poisson distributions is plotted in Fig. 8 as a function of Φ/π. If we denote $[\Phi]$ as $\Phi \bmod 2\pi$ such that $-\pi \leq [\Phi] \leq \pi$, then, under the near in-phase condition for Poisson height distribution,

$$C(k_\perp,r) \approx e^{-(1/2)H(r)[\Phi]^2}, \qquad (26)$$

which is the same as for Gaussian height distribution.[21] In Fig. 9 we plot the height difference function $C(k_\perp,r)$ for both distributions as a function of r. Even in the case of $\Omega \gg 1$ for the continuous surface, as long as the near in-phase condition is satisfied, $C(k_\perp,r)$ for both distributions are the same. Under the near out-of-phase condition for the Poisson distribution

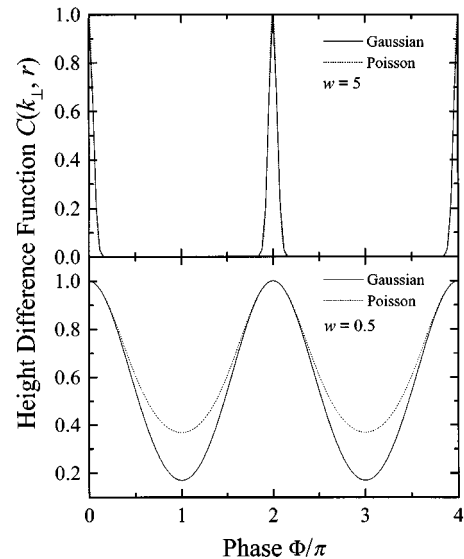$$C(k_\perp,r) \approx e^{-2H(r)+(1/2)H(r)(\pi-|[\Phi]|)^2}. \qquad (27)$$

FIG. 8. Oscillatory behavior of the height difference function $C(k_\perp,r)$ as a function of phase Φ in the discrete lattice case for different height distributions and interface widths.
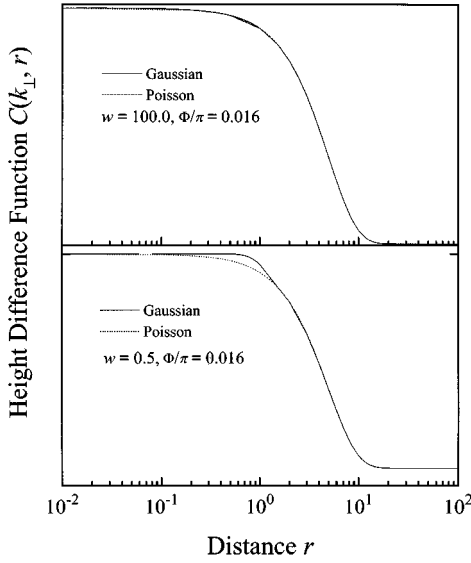
FIG. 9. Height difference function $C(k_\perp,r)$ for different height distributions under the near in-phase condition.

This equation is different from that obtained from the Gaussian distribution[21]

$$C(k_\perp,r) \approx e^{(1/2)H(r)[\Phi]^2} + e^{-(1/2)H(r)(2\pi-[\Phi]^2)}. \quad (28)$$

Figure 10 shows the difference between these two distributions. Notice that for the case of $(k_\perp w)^2 \ll 1$, which is $\Omega \ll 1$ for the continuous surface, as long as the near out-of-phase condition is satisfied, $C(k_\perp,r)$ for both distributions are different. The deviation in the oscillation behavior in Fig. 8 for different height distributions also originates from Eqs. (27) and (28).

B. The diffraction profile $S(\mathbf{k})$

The height difference function $C(k_\perp,r)$ can be broken into two parts
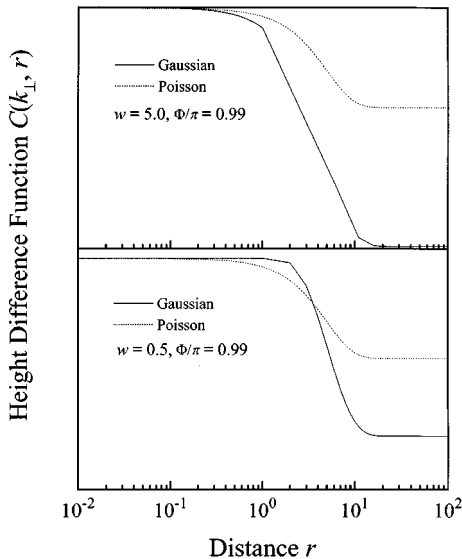

FIG. 10. Height difference function $C(k_\perp,r)$ for different height distributions under the near out-of-phase condition.

$$C(k_\perp,r) = C(k_\perp,\infty) + \Delta C(k_\perp,r), \quad (29)$$

where $C(k_\perp,\infty) = \lim_{r\to\infty} C(k_\perp,r)$. As $\lim_{r\to\infty} R(r) = 0$, only the zeroth-order term in Eq. (20) survives. For classic orthogonal polynomials $Q_0 = 1$, $h_0^2 = 1$, and $\lambda_0 = 0$, we have

$$C(k_\perp,\infty) = \left| \int f(x) e^{ik_\perp x} dx \right|^2. \quad (30)$$

Therefore, the diffraction profile $S(\mathbf{k}_\parallel)$ can be written as

$$S(\mathbf{k}_\parallel) = S_\delta(\mathbf{k}_\parallel,k_\perp) + S_{\text{diff}}(\mathbf{k}_\parallel,k_\perp), \quad (31)$$

where

$$S_\delta(\mathbf{k}_\parallel,k_\perp) = (2\pi)^2 C(k_\perp,\infty) \delta(\mathbf{k}_\parallel)$$

$$= (2\pi)^2 \left| \int f(x) e^{ik_\perp x} dx \right|^2 \delta(\mathbf{k}_\parallel) \quad (32)$$

and

$$S_{\text{diff}}(\mathbf{k}_\parallel,k_\perp) = \int\int e^{i\mathbf{k}_\parallel \cdot \mathbf{r}} d^2 r \sum_{n=1}^{\infty} \frac{R(r)^{\lambda_n/\lambda_1}}{h_n^2}$$

$$\times \left| \int f(x) Q_n(x) e^{ik_\perp x} dx \right|^2$$

$$= \sum_{n=1}^{\infty} \frac{1}{h_n^2} \left| \int f(x) Q_n(x) e^{ik_\perp x} dx \right|^2$$

$$\times \int\int R(r)^{\lambda_n/\lambda_1} e^{i\mathbf{k}_\parallel \cdot \mathbf{r}} d^2 r. \quad (33)$$

From Eqs. (32) and (33), it is clear that the δ-peak intensity of the diffraction profile depends on the characteristic function of the surface height distribution and the diffuse profile depends on both the distribution and the correlation functions of surface height. If we think of the total diffuse profile as the sum of many small diffuse profiles, then for each small diffuse profile, the surface height distribution $f(x)$ determines the peak intensity and the correlation function $R(r)$ determines the shape of the diffuse profile.

1. The intensity of the δ peak

The δ-peak intensity is proportional to the square modulus of the characteristic function of the height distribution $f(x)$. For different height distributions, the δ-peak intensity has a different relation to $k_\perp$, as seen in Table II. As

$$\int f(x) e^{ik_\perp x} dx = \sum_{m=0}^{\infty} \frac{\nu_m}{m!} (ik_\perp)^m, \quad (34)$$

where ν_m is the mth-order moment of $f(x)$ about the origin, we have

$$C(k_\perp,\infty) = \left[\sum_{m=0}^{\infty} (-1)^m \frac{\nu_{2m}}{(2m)!} k_\perp^{2m} \right]^2$$

$$+ \left[\sum_{m=0}^{\infty} (-1)^m \frac{\nu_{2m+1}}{(2m+1)!} k_\perp^{2m+1} \right]^2. \quad (35)$$

For symmetric height distributions about zero, only the first term on the right-hand side exists. But for asymmetric height

TABLE II. δ-peak intensity for different height distributions.

Distribution	δ-peak intensity
Gaussian	$\exp(-k_\perp^2 w^2)$
exponential	$\dfrac{1}{1+k_\perp^2 w^2}$
Γ	$\dfrac{1}{(1+k_\perp^2 \sigma^2)^{\kappa+1}}$
uniform	$\dfrac{\sin^2(k_\perp a)}{k_\perp^2 a^2}$
Rayleigh	$\left\| {}_1F_1\left(\dfrac{1}{2},\dfrac{1}{2};-\dfrac{k_\perp^2 \sigma^2}{2}\right)\right\|^2$

distributions, the second term, i.e., the odd terms on the right-hand side, should be taken into account. If $\langle x \rangle = 0$ for $\Omega < 1$, the δ-peak intensity can be written as

$$C(k_\perp,\infty) \approx (1 - \tfrac{1}{2}k_\perp^2 w^2 + \tfrac{1}{24}\kappa_4 k_\perp^4 w^4 - \tfrac{1}{720}\kappa_6 k_\perp^6 w^6)^2$$
$$+ \tfrac{1}{36}\kappa_3^2 k_\perp^6 w^6$$
$$\approx 1 - k_\perp^2 w^2 + (\tfrac{1}{4} + \tfrac{1}{12}\kappa_4)k_\perp^4 w^4 + (\tfrac{1}{36}\kappa_3^2 - \tfrac{1}{24}\kappa_4$$
$$- \tfrac{1}{360}\kappa_6)k_\perp^6 w^6, \qquad (36)$$

where $\kappa_m = \nu_m / w^m$ for $m > 2$. κ_3 is called the skewness and κ_4 is called the kurtosis. The more asymmetric the height distribution, the greater the contribution from the odd moments and the more deviation from the Gaussian distribution.

The total integrated intensity of the δ peak I_δ is

$$I_\delta = \int S_\delta(\mathbf{k}_\parallel, k_\perp)d^2 k_\parallel = (2\pi)^2 \left| \int f(x)e^{ik_\perp x}dx \right|^2. \quad (37)$$

Figure 11 shows the δ-peak intensity as a function of Ω for different distributions. For the Γ distribution, as κ becomes larger and larger, the distribution is more like a Gaussian
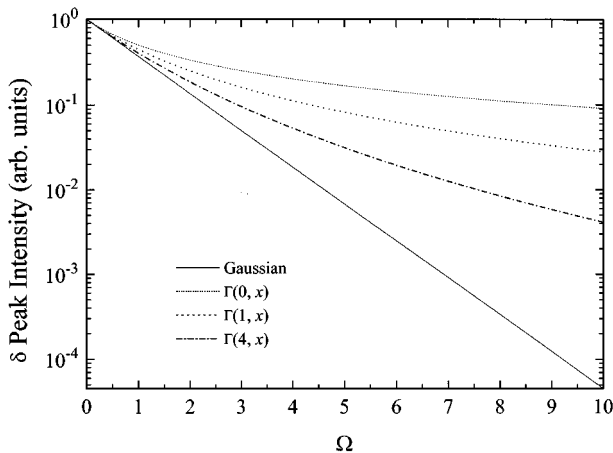

FIG. 11. δ-peak intensity versus Ω ($=k_\perp^2 w^2$) for different height distributions.

distribution and the results are closer to that obtained from the Gaussian distribution. The total integrated intensity I of the whole scattering field is

$$I = \int S(\mathbf{k}_\parallel, k_\perp)d^2 k_\parallel = (2\pi)^2. \qquad (38)$$

Then

$$R_\delta = \frac{I_\delta}{I} = \left| \int f(x)e^{ik_\perp x}dx \right|^2 \qquad (39)$$

and

$$R_{\text{diff}} = 1 - \frac{I_\delta}{I} = 1 - \left| \int f(x)e^{ik_\perp x}dx \right|^2. \qquad (40)$$

One often uses R_δ to determine interface width w through the relation[3]

$$R_\delta = e^{-k_\perp^2 w^2}, \qquad (41)$$

which was derived based on the assumption of a Gaussian height distribution. However, in general, the relation between R_δ and w also depends on the height distribution as seen from Table II and Fig. 11. If the surface height no longer has a Gaussian distribution, Eq. (41) should be modified according to the height characteristic function. Only when $\Omega \ll 1$, Eq. (41) approximately holds for all kinds of distributions and R_δ has the same result for different distributions.

In fact, we can extend Eqs. (39) and (40) to a surface with any height distribution as long as the surface is self-affine. As $r \to \infty$, $R \to 0$, which means that x and y are two independent random variables but the associated distribution functions $f(x)$ and $f(y)$ are the same. So the joint distribution can be simply written as

$$f^J(x,y;R \to 0) = f(x)f(y). \qquad (42)$$

Therefore, Eqs. (39) and (40) exist for any self-affine surface with an arbitrary height distribution. Equation (39) shows that R_δ actually is only related to the characteristic function of the surface height distribution. Then two important results can be drawn from the discussion above.

(i) If we assume that the surface height distribution is a symmetric distribution, Eq. (39) becomes

$$R_\delta(k_\perp) = \left| \int f(x)\cos(k_\perp x)dx \right|^2. \qquad (43)$$

By changing the incident angle of the incoming beam with respect to the surface normal, the $k_\perp$ changes correspondingly and one can obtain the characteristic function of the height distribution through Eq. (43). Then an inverse Fourier cosine transformation of the characteristic function $R_\delta(k_\perp)^{1/2}$ will give the surface height distribution. This gives a possible way to obtain the surface height distribution by diffraction.

(ii) Equation (39) also gives us a method to determine whether or not the surface height obeys a Gaussian distribution. Since for a surface with Gaussian distribution the characteristic function is also a Gaussian function with respect to $k_\perp$ [Eq. (41)], one can always plot $\log[R_\delta(k_\perp)]$ versus $k_\perp^2$ in a

linear coordinate. If the plot is a straight line, the height distribution should be a Gaussian distribution; otherwise, it is a non-Gaussian distribution.

2. Diffuse profile

Equation (33) can be written as

$$S_{\text{diff}} = 2\pi \sum_{n=1}^{\infty} \frac{1}{h_n^2} \left| \int f(x) Q_n(x) e^{ik_\perp x} dx \right|^2$$

$$\times \int_0^{\infty} r\, R(r)^{\lambda_n/\lambda_1} J_0(k_\| r) dr. \tag{44}$$

Two cases should be discussed: $\Omega \ll 1$ and $\Omega \gg 1$.

(a) $\Omega \ll 1$. For $\Omega \ll 1$, first we need to prove that

$$\left| \int f(x) Q_n(x) e^{ik_\perp x} dx \right|^2 \sim O(\Omega^n). \tag{45}$$

It is well known that for general orthogonal polynomials, an arbitrary polynomial of nth degree can be expressed as a linear combination of $Q_0(x)$, $Q_1(x), \ldots, Q_n(x)$.[25] Then

$$\int f(x) Q_n(x) e^{ik_\perp x} dx$$

$$= \sum_{m=0}^{\infty} \frac{(ik_\perp)^m}{m!} \int f(x) Q_n(x) x^m dx$$

$$= \sum_{m=n}^{\infty} \frac{(ik_\perp)^m}{m!} \int f(x) Q_n(x) x^m dx$$

$$= \sum_{m=0}^{\infty} \frac{(ik_\perp)^{n+m}}{(n+m)!} \sum_{j=0}^{n} a_j \int f(x) x^{n+j+m} dx$$

$$= \sum_{m=0}^{\infty} \sum_{j=0}^{n} \frac{(ik)^{n+m}}{(n+m)!} a_j \nu_{n+j+m},$$

where ν_k is the kth-order moment of $f(x)$. Since

$$\nu_k = \kappa_k w^k, \tag{46}$$

$|\int f(x) Q_n(x) e^{ik_\perp x} dx|^2 \sim O(\Omega^n)$. Then for $\Omega \ll 1$, the diffuse profile

$$S_{\text{diff}} \approx \frac{2\pi}{h_1^2} \left| \int f(x) Q_1(x) e^{ik_\perp x} dx \right|^2 \int_0^{\infty} r\, R(r) J_0(k_\| r) dr. \tag{47}$$

The shape of the diffuse profile is mainly determined by the integral $\int_0^{\infty} r\, R(r) J_0(k_\| r) dr$, which is proportional to the power spectrum $\langle |h(k_\|)|^2 \rangle$ of the surface height and has nothing to do with the surface height distribution. For a self-affine surface, a K-correlation model proposed by Palasant-zas gives[28]

$$\langle |h(k_\|)|^2 \rangle = \frac{A}{(2\pi)^5} \frac{w^2 \xi^2}{(1+bk_\|^2 \xi^2)^{1+\alpha}}, \tag{48}$$

where A is the surface area and $b = [1-(1+bQ_c^2\xi^2)^{-\alpha}]/2\alpha$. Here Q_c is the stopping frequency due to the atomic spacing. Equation (48) shows that the full width

TABLE III. Diffuse peak intensity for different height distributions ($\Omega \ll 1$).

Distribution	Diffuse peak intensity
Gaussian	$k_\perp^2 w^2 \xi^2 \exp(-k_\perp^2 w^2)$
exponential	$\dfrac{k_\perp^2 w^2 \xi^2}{(1+k_\perp^2 w^2)^2}$
Γ	$(\kappa+1)\dfrac{k_\perp^2 \sigma^2 \xi^2}{(1+k_\perp^2 \sigma^2)^{\kappa+2}}$
uniform	$\dfrac{3\pi\xi^2}{2k_\perp a} J_{3/2}^2(k_\perp a)$
Rayleigh	$\dfrac{\pi}{8} k_\perp^2 \sigma^2 \xi^2 \, _2F_2\left(\dfrac{3}{2},\dfrac{3}{2};\dfrac{3}{2},\dfrac{1}{2};-\dfrac{k_\perp^2 \sigma^2}{2}\right)$

at half maximum (FWHM) of the diffuse profile is inversely proportional to the lateral correlation length ξ, and for $k_\| \gg 1$,

$$\langle |h(k_\|)|^2 \rangle \propto k_\|^{-2-2\alpha}. \tag{49}$$

Equation (48) gives the possibility of determining ξ and α through the diffuse profile.

However, the diffuse peak intensity depends on the specific height distributions as listed in Table III. In fact, Eq. (47) shows that the diffuse peak intensity is the square modulus of the product of the surface height characteristic function and its first-order derivative.

(b) $\Omega \gg 1$. In this case, other terms in the summation of Eq. (33) will affect the diffuse profile. If we assume a self-affine surface and express $R(r)$ as $e^{-(r/\xi)^{2\alpha}}$, then for both the Gaussian distribution and the Γ distribution, as $\lambda_n = n$, we have

$$\int_0^{\infty} r\, R(r)^n J_0(k_\| r) dr$$

$$= \xi^2 n^{-1/\alpha} \int_0^{\infty} X \exp(-X^{2\alpha}) J_0(k_\| \xi n^{-1/2\alpha} X) dX$$

$$= \xi^2 n^{-1/\alpha} \int_0^{\infty} X \exp(-X^{2\alpha}) dX$$

$$\times \sum_{m=0}^{\infty} \frac{(-1)^m}{(m!)^2} \left(\frac{k_\| \xi X}{2}\right)^{2m} n^{-m/\alpha}; \tag{50}$$

so

$$S_{\text{diff}} = 2\pi \xi^2 \sum_{m=0}^{\infty} \frac{(-1)^m}{(m!)^2} \int_0^{\infty} X \exp(-X^{2\alpha}) \left(\frac{k_\| \xi X}{2}\right)^{2m} dX$$

$$\times \left[\sum_{n=1}^{\infty} \frac{1}{h_n^2} n^{-(m+1)/\alpha} \left| \int f(x) Q_n(x) e^{ik_\perp x} dx \right|^2 \right]. \tag{51}$$

The asymptotic form for summation in the square brackets is different for different height distributions. For Gaussian height distribution[21]

$$[\quad]=\sum_{n=1}^{\infty}\frac{n^{-(m+1)/\alpha}}{n!}(k_{\perp}^2 w^2)^n \exp(-k_{\perp}^2 w^2)$$

$$\approx (k_{\perp}^2 w^2)^{-(m+1)/\alpha} \quad \text{for } \Omega \gg 1. \tag{52}$$

Then

$$S_{\text{diff}} \approx 2\pi\xi^2 \Omega^{-1/\alpha} \int_0^{\infty} X \exp(-X^{2\alpha}) J_0(k_{\parallel}\xi\Omega^{-1/2\alpha}X)dX. \tag{53}$$

For the exponential height distribution

$$[\quad]=\sum_{n=1}^{\infty}\frac{(k_{\perp}^2 w^2)^n}{(1+k_{\perp}^2 w^2)^{n+1}} n^{-(m+1)/\alpha}$$

$$\approx \frac{1}{1+k_{\perp}^2 w^2}\sum_{n=1}^{\infty} n^{-(m+1)/\alpha}=\frac{1}{1+\Omega}\zeta\left(\frac{m+1}{\alpha}\right), \tag{54}$$

where $\zeta(x)$ is the Riemann zeta function. For $x \gg 1$ one has[29]

$$\zeta(x)\approx 2^{-x}+1, \tag{55}$$

which leads to

$$S_{\text{diff}}\approx \frac{2\pi\xi^2}{1+\Omega}\left[\int_0^{\infty} X \exp(-X^{2\alpha})J_0(k_{\parallel}\xi X)dX \right.$$

$$\left. +2^{-1/\alpha}\int_0^{\infty} X \exp(-X^{2\alpha})J_0(2^{-1/2\alpha}k_{\parallel}\xi X)dX\right]. \tag{56}$$

It is clear that different height distributions give different asymptotic results. For Gaussian distribution, the diffuse peak intensity $I_D \propto (k_{\perp})^{-2/\alpha}$ and also the FWHM is proportional to $(k_{\perp})^{1/\alpha}$. Due to these two relations, one can derive the roughness exponent α. However, for exponential height distribution, there is no such relation and one cannot obtain α using these relations obtained from Gaussian distribution. Figure 12 shows the FWHM of the diffuse profile as a function of $k_{\perp}$ for different α values and for different height distributions. Here we assume that $w=0.5$ and $\xi=5.0$. For $k_{\perp} \ll 1$ both the Gaussian height distribution and the exponential distribution give the same FWHM, while for $k_{\perp} \gg 1$ they have different behaviors. For the Gaussian distribution, the FWHM diverges as $k_{\perp}$ goes to infinity; for the exponential distribution, the FWHM will be bounded by a certain value. These results show that caution should be taken when one wants to determine α through the relations obtained under the assumption of the Gaussian height distribution.

IV. CONCLUSION

One question is immediately raised here: How accurate can the diffraction technique be used to estimate the growth kinetics without the knowledge of the surface height distribution? For $\Omega \ll 1$, as roughness parameters individually affect the density and shape of the diffraction profiles, one can obtain the interface width w, lateral correlation length ξ, and
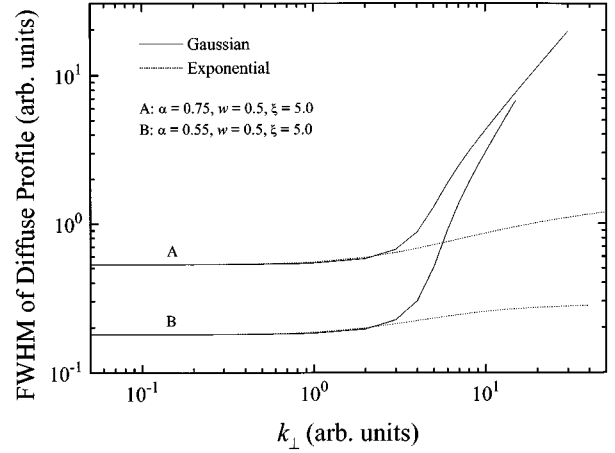

FIG. 12. FWHM of the diffuse profile versus $k_{\perp}$ for different height distributions.

roughness exponent α through Eqs. (41), (48), and (49) without any specific assumption about the surface height distribution. However, for $\Omega \gg 1$, as the diffuse profile depends on both the surface height distribution and the correlation function, the relations between roughness parameters and diffraction profiles are much more complicated and depend very much on the surface height distribution. There is no general way to determine the roughness parameters.

If one uses the inverse Fourier transform to determine the height-height correlation function $H(r)$ from the diffraction profiles,[30] the same problem also can arise since different height distributions give different forms of $C(k_{\perp},r)$, as discussed above. However, for $\Omega \ll 1$ the approximation $C(k_{\perp},r)\approx 1-\frac{1}{2}k_{\perp}^2 H(r)$ always holds without any specific assumption about the height distribution and one can obtain the height-height correlation function directly without the knowledge of the distribution.

APPENDIX A

A general single variable Langevin equation takes the form[31]

$$\frac{dx}{dr}=h(x,r)+g(x,r)\eta(r), \tag{A1}$$

where $\eta(r)$ is a Gaussian-Markov process, satisfying

$$\langle\eta(r)\rangle=0, \tag{A2}$$

$$\langle\eta(r)\eta(r')\rangle=2\delta(r-r').$$

Here we adopt the Stratonovich interpretation of Eq. (A1). The corresponding Fokker-Planck equation for Eq. (A1) is

$$\frac{\partial P(x|x_0;r)}{\partial r} = -\frac{\partial}{\partial x}[A(x,r)P(x|x_0;r)]$$

$$+\frac{\partial^2}{\partial x^2}[B(x,r)P(x|x_0;r)], \qquad (A3)$$

where

$$A(x,r) = h(x,r) + g(x,r)\frac{\partial g(x,r)}{\partial x}, \qquad (A4)$$

$$B(x,r) = g^2(x,r), \qquad (A5)$$

$P(x|x_0;r)$ is the condition probability density, and x and x_0 are separated by distance r. We now consider the solution of Eq. (A3) corresponding to an initial value

$$P(x|x_0;r=0) = \delta(x-x_0) \qquad (A6)$$

and the reflecting barriers boundary conditions

$$\frac{\partial}{\partial x}[B(x,r)P] - A(x,r)P = 0 \quad \text{at } x = x_1,x_2. \qquad (A7)$$

A further assumption can be made concerning coefficients $A(x,r)$ and $B(x,r)$:

$$A(x,r) = A(x)F(r), \qquad (A8)$$

$$B(x,r) = B(x)F(r).$$

Then Eq. (A3) can be solved by a separation of variables. Let

$$P(x|x_0;r) = X(x)T(r). \qquad (A9)$$

We have

$$\frac{dT}{dr} = -\lambda F(r)T(r), \qquad (A10)$$

$$\frac{d^2}{dx^2}[B(x)X(x)] - \frac{d}{dx}[A(x)X(x)] + \lambda X(x) = 0. \qquad (A11)$$

The solution for Eq. (A10) is obvious:

$$T(r) = T(0)\exp\left(-\lambda\int_0^r F(r)dr\right). \qquad (A12)$$

Equation (A11) is an eigenvalue problem of the second-order ordinary differential equation. We can give some special form of $A(x)$ and $B(x)$ and Eq. (A11) can be changed to a Sturm-Liouville equation. Let

$$B(x) = \beta(cx^2 + dx + e), \qquad (A13)$$

$$A(x) = \frac{dB(x)}{dx} + \beta(ax + b), \qquad (A14)$$

and

$$\frac{dW(x)}{dx} = \frac{ax+b}{cx^2+dx+c}W(x) \quad \text{(Pearson equation)}. \qquad (A15)$$

Then Eq. (A11) becomes a standard Sturm-Liouville equation

$$\frac{d}{dx}\left[B(x)W(x)\frac{dX}{dx}\right] + \lambda W(x)X = 0 \qquad (A16)$$

and the boundary condition is

$$B(x)W(x)\frac{dX}{dx} = 0, \quad x = x_1,x_2. \qquad (A17)$$

So the general solution for Eq. (A3) is

$$P(x|x_0;r) = W(x)\sum_n \exp\left(-\lambda_n\int_0^r F(r)dr\right)Q_n(x)Q_n(x_0), \qquad (A18)$$

where $Q_n(x)$ is the eigenfunction of Eqs. (A16) and (A17) and λ_n is the corresponding eigenvalue. Q_n satisfies the normalized relation

$$\int_{x_1}^{x_2} W(x)Q_n(x)Q_m(x)dx = \delta_{nm}. \qquad (A19)$$

In fact, $Q_n(x)$ is the classical orthogonal polynomial. If the probability density for x_0 is given as $W(x_0)$, then the joint distribution for x and x_0 is

$$P(x,x_0;r) = W(x)W(x_0)\sum_n \bar{R}^{\lambda_n}Q_n(x)Q_n(x_0), \qquad (A20)$$

where

$$\bar{R}(r) = \exp\left(-\int_0^r F(r)dr\right). \qquad (A21)$$

The correlation function $R(r)$ is given as

$$R(r) = \bar{R}(r)^{\lambda_1}. \qquad (A22)$$

APPENDIX B

The individual height distributions are discussed below.

1. Continuous surfaces

(a) Gaussian distribution

If the surface height obeys the Gaussian distribution,

$$f(x) = \frac{1}{\sqrt{2\pi}w}\exp\left(-\frac{x^2}{2w^2}\right). \qquad (B1)$$

Equation (B1) is the weighting function of Hermite polynomials $H_n(x)$:

$$\int_{-\infty}^{\infty}\frac{1}{\sqrt{2\pi}w}\exp\left(-\frac{x^2}{2w^2}\right)H_n\left(\frac{x}{\sqrt{2}w}\right)H_m\left(\frac{x}{\sqrt{2}w}\right)dx$$

$$= 2^n n!\,\delta_{nm}, \qquad (B2)$$

e.g.,

$$h_n^2 = 2^n n!. \qquad (B3)$$

The eigenvalue $\lambda_n = n$. So

$$f^J(x,y;R) = \frac{1}{2\pi w^2} \exp\left(-\frac{x^2+y^2}{2w^2}\right)$$

$$\times \sum_{n=0}^{\infty} \frac{R^n}{2^n n!} H_n\left(\frac{x}{\sqrt{2}w}\right) H_n\left(\frac{y}{\sqrt{2}w}\right). \qquad (B4)$$

As

$$\sum_{n=0}^{\infty} \frac{t^n}{2^n n!} H_n(x)H_n(y)$$

$$= (1-t^2)^{-1/2} \exp\left(\frac{2xyt-(x^2+y^2)t^2}{1-t^2}\right), \qquad (B5)$$

the joint distribution for Gaussian height distribution is

$$f^J(x,y;R) = \frac{1}{2\pi w^2\sqrt{1-R^2}} \exp\left(-\frac{x^2+y^2-2xyR}{2w^2(1-R^2)}\right). \qquad (B6)$$

This is the well-known joint distribution function for Gaussian process. According to Eq. (5), the height difference distribution is

$$p(z,r) = \frac{1}{2w\sqrt{\pi(1-R)}} \exp\left(-\frac{z^2}{4w^2(1-R)}\right). \qquad (B7)$$

Equation (B7) indicates that the height difference z also obeys the Gaussian distribution. From the definition of height-height correlation function $H(r)$,

$$H(r) = \langle[h(\mathbf{r})-h(0)]^2\rangle = 2w^2(1-R), \qquad (B8)$$

one has

$$p(z,r) = \frac{1}{\sqrt{2\pi H(r)}} \exp\left(-\frac{z^2}{2H(r)}\right) \qquad (B9)$$

and the height difference function

$$C(k_\perp,r) = \exp\left[-\tfrac{1}{2}k_\perp^2 H(r)\right]. \qquad (B10)$$

(b) Exponential distribution

The exponential distribution

$$f(x) = \frac{1}{w} \exp\left(-\frac{x}{w}\right), \quad x \geq 0. \qquad (B11)$$

This is an asymmetric distribution and its corresponding orthogonal polynomials are Laguerre polynomials $L_n(x)$:

$$h_n^2 = \int_0^{\infty} \frac{1}{w} \exp\left(-\frac{x}{w}\right) L_n\left(\frac{x}{w}\right) L_n\left(\frac{x}{w}\right) dx = 1. \qquad (B12)$$

The corresponding eigenvalue $\lambda_n = n$. Therefore,

$$f^J(x,y;R) = \frac{1}{w^2} \exp\left(-\frac{x+y}{w}\right) \sum_{n=0}^{\infty} R^n L_n\left(\frac{x}{w}\right) L_n\left(\frac{y}{w}\right). \qquad (B13)$$

As

$$\sum_{n=0}^{\infty} L_n(x)L_n(y)t^n = \frac{1}{1-t} \exp\left(-t\frac{x+y}{1-t}\right) I_0\left(\frac{2\sqrt{xyt}}{1-t}\right), \qquad (B14)$$

where $I_0(x)$ is the zeroth-order modified Bessel function. Then

$$f^J(x,y;R) = \frac{1}{w^2(1-R)} \exp\left(-\frac{x+y}{w(1-R)}\right) I_0\left(\frac{2\sqrt{xyR}}{w(1-R)}\right). \qquad (B15)$$

Therefore,

$$p(z,r) = \int_0^{\infty} \frac{1}{w^2(1-R)} \exp\left(-\frac{z+2y}{w(1-R)}\right)$$

$$\times I_0\left(\frac{2\sqrt{(y+z)yR}}{w(1-R)}\right) dy$$

$$= \frac{1}{2w\sqrt{1-R}} \exp\left(-\frac{|z|}{\sigma\sqrt{1-R}}\right), \qquad (B16)$$

i.e.,

$$p(z,r) = \frac{1}{2w\sqrt{1-R}} \exp\left(-\frac{|z|}{w\sqrt{1-R}}\right), \quad -\infty \leq z \leq \infty. \qquad (B17)$$

This means that the height difference distribution is still exponential, but it becomes symmetric. In this case,

$$C(k_\perp,r) = \frac{1}{1+\tfrac{1}{2}k_\perp^2 H(r)}. \qquad (B18)$$

This is different from that of the Gaussian distribution.

(c) Γ distribution

The Γ distribution

$$f(x) = \frac{1}{\Gamma(\kappa+1)\sigma^{\kappa+1}} x^\kappa e^{-x/\sigma}, \quad x \geq 0. \qquad (B19)$$

This is the weighting function of associated Laguerre polynomials:

$$h_n^2 = \int_0^{\infty} \frac{1}{\Gamma(\kappa+1)\sigma^{\kappa+1}} x^\kappa \exp\left(-\frac{x}{\sigma}\right) L_n^{(\kappa)}\left(\frac{x}{\sigma}\right) L_n^{(\kappa)}\left(\frac{x}{\sigma}\right) dx$$

$$= \frac{\Gamma(n+\kappa+1)}{\Gamma(\kappa+1)\Gamma(n+1)}. \qquad (B20)$$

The corresponding eigenvalue $\lambda_n = n$. The joint distribution is

$$f^J(x,y;R) = \frac{1}{\Gamma(\kappa+1)\sigma^{2\kappa+2}} (xy)^\kappa \exp\left(-\frac{x+y}{\sigma}\right)$$

$$\times \sum_{n=0}^{\infty} \frac{\Gamma(n+1)}{\Gamma(n+\kappa+1)} R^n L_n^{(\kappa)}\left(\frac{x}{\sigma}\right) L_n^{(\kappa)}\left(\frac{y}{\sigma}\right) \qquad (B21)$$

and

$$\sum_{n=0}^{\infty} \frac{\Gamma(n+1)R^n}{\Gamma(n+\kappa+1)} L_n^{(\kappa)}(x)L_n^{(\kappa)}(y)$$

$$= \frac{1}{(xyR)^{\kappa/2}(1-R)} \exp\left(-R\frac{x+y}{1-R}\right)I_\kappa\left(\frac{2\sqrt{xyR}}{1-R}\right), \tag{B22}$$

where $I_\kappa(x)$ is the κth-order modified Bessel function. Then

$$f^J(x,y;R) = \frac{1}{\Gamma(\kappa+1)\sigma^{\kappa+2}(1-R)R^{\kappa/2}}(xy)^{\kappa/2}$$

$$\times \exp\left(-\frac{x+y}{\sigma(1-R)}\right)I_\kappa\left(\frac{2\sqrt{xyR}}{\sigma(1-R)}\right). \tag{B23}$$

The height difference distribution is calculated as

$$p(z,r) = \frac{1}{\Gamma(\kappa+1)\sigma\sqrt{\pi}(1-R)^{\kappa+1}}\left(\frac{z\sqrt{1-R}}{2\sigma}\right)^{\kappa+1/2}$$

$$\times K_{\kappa+1/2}\left(\frac{z}{\sigma\sqrt{1-R}}\right), \tag{B24}$$

where K_ν is a modified Bessel function. The height difference function is then

$$C(k_\perp,r) = \frac{1}{[1+k_\perp^2\sigma^2(1-R)]^{\kappa+1}}. \tag{B25}$$

Note that for this distribution, the interface width w is expressed as

$$w^2 = (\kappa+1)\sigma^2. \tag{B26}$$

Therefore,

$$C(k_\perp,r) = \frac{1}{\left(1+\frac{k_\perp^2 H(r)}{2(\kappa+1)}\right)^{\kappa+1}}. \tag{B27}$$

The exponential distribution is a special case when $\kappa=0$.

(d) Rayleigh distribution

The Rayleigh distribution

$$f(x) = \frac{x}{w^2}\exp\left(-\frac{x^2}{2w^2}\right), \quad x\geq0. \tag{B28}$$

This is also an asymmetric distribution. The corresponding orthogonal polynomials are Laguerre polynomials $L_n(x)$:

$$h_n^2 = \int_0^\infty \frac{x}{w^2}\exp\left(-\frac{x^2}{2w^2}\right)L_n\left(\frac{x^2}{2w^2}\right)L_n\left(\frac{x^2}{2w^2}\right)dx = 1. \tag{B29}$$

The joint distribution is

$$f^J(x,y;R) = \frac{xy}{\sigma^4}\exp\left(-\frac{x^2+y^2}{2\sigma^2}\right)\sum_{n=0}^{\infty}R^n L_n\left(\frac{x^2}{2\sigma^2}\right)L_n\left(\frac{y^2}{2\sigma^2}\right). \tag{B30}$$

According to Eq. (B14),

$$f^J(x,y;R) = \frac{xy}{w^4(1-R)}\exp\left(-\frac{x^2+y^2}{w^2(1-R)}\right)I_0\left(\frac{2xy\sqrt{R}}{w^2(1-R)}\right). \tag{B31}$$

Therefore,

$$p(z,r) = \int_0^\infty \frac{y(y+z)}{w^4(1-R)}\exp\left(-\frac{y^2+(z+y)^2}{2w^2(1-R)}\right)$$

$$\times I_0\left(\frac{y(y+z)\sqrt{R}}{w^2(1-R)}\right)dy \tag{B32}$$

and

$$C(k_\perp,r) = \sum_{n=0}^{\infty}\frac{\pi k_\perp w^2}{2}\left[\left(-\frac{1}{2}\right)_n\right]^2$$

$$\times R^n\,{}_2F_2\left(\frac{3}{2},\frac{3}{2};\frac{3}{2},\frac{3}{2}-n;-\frac{k_\perp^2 w^2}{2}\right), \tag{B33}$$

where ${}_2F_2(\alpha;\beta;\gamma;\eta;z)$ is a hypergeometric function.

(e) Uniform distribution

The uniform distribution

$$f(x) = \frac{1}{2a}, \quad -a\leq x\leq a. \tag{B34}$$

The corresponding polynomials are Legendre polynomials $P_n(x)$:

$$h_n^2 = \int_{-a}^{a}\frac{1}{2a}P_n\left(\frac{x}{a}\right)P_n\left(\frac{x}{a}\right)dx = \frac{1}{2a}. \tag{B35}$$

The corresponding eigenvalue $\lambda_n = n(n+1)$. The joint distribution is

$$f^J(x,y;R) = \frac{1}{4a^2}\sum_{n=0}^{\infty}(2n+1)R^{n(n+1)/2}P_n\left(\frac{x}{a}\right)P_n\left(\frac{y}{a}\right). \tag{B36}$$

The height difference distribution is

$$p(z,r) = \frac{1}{4a^2}\sum_{n=0}^{\infty}(2n+1)R^{n(n+1)/2}$$

$$\times \int_{x_1}^{x_2}P_n\left(\frac{y+z}{a}\right)P_n\left(\frac{y}{a}\right)dy, \tag{B37}$$

where x_1 and x_2 are the integration boundaries: $x_1 = \max[-a-z,-a]$ and $x_2 = \min[a-z,a]$. The range of z is from $-2a$ to $2a$. The height difference function is therefore

$$C(k_\perp,r)=\frac{\pi}{2k_\perp a}\sum_{n=0}^{\infty}(2n+1)R^{n(n+1)/2}J_{n+1/2}^2(k_\perp a).$$
$$(B38)$$

2. Discrete surface

We consider the Poisson distribution

$$f(x)=\frac{e^{-a}a^x}{x!},\quad x=0,1,2,\ldots,\quad a>0.\qquad(B39)$$

The corresponding orthogonal polynomials are Charlier polynomials, defined as[32]

$$C_n(x,a)=a^{-n}L_n^{(x-n)}(a),\qquad(B40)$$

where $L_n^{(x-n)}(a)$ is associated Laguerre polynomial. The orthogonal relation is given by

$$\sum_{x=0}^{\infty}f(x)C_n(x,a)C_m(x,a)=\frac{a^{-n}}{n!}\,\delta_{nm}.\qquad(B41)$$

Therefore,

$$h_n^2=\frac{a^{-n}}{n!}.\qquad(B42)$$

The joint distribution function is

$$f^J(x,y;R)=\frac{e^{-2a}a^{x+y}}{x!y!}\sum_{n=0}^{\infty}\left(\frac{R}{a}\right)^n n!L_n^{(x-n)}(a)L_n^{(y-n)}(a)$$
$$(B43)$$

and

$$\sum_{k=0}^{\infty}k!t^kL_k^{(\alpha-k)}(x)L_k^{(\beta-k)}(y)$$

$$=\beta!t^\beta(1-ty)^{\alpha-\beta}e^{txy}L_\beta^{(\alpha-\beta)}\left(-\frac{(1-tx)(1-ty)}{t}\right).$$
$$(B44)$$

Therefore,

$$f^J(x,y;R)=\frac{e^{-2a}a^x}{x!}R^y(1-R)^{x-y}e^{aR}L_y^{(x-y)}\left(-\frac{a(1-R)^2}{R}\right).$$
$$(B45)$$

The height difference distribution $f(z;R)$ can be written as

$$p(z,r)=\sum_{y=0}^{\infty}f(z+y,y;R)$$

$$=\frac{e^{-2a+aR}(1-R)^2a^z}{z!}\sum_{y=0}^{\infty}\frac{(aR)^y}{(z+1)_y}L_y^z$$

$$\times\left(-\frac{a(1-R)^2}{R}\right).\qquad(B46)$$

Since

$$\sum_{k=0}^{\infty}\frac{t^k}{(\alpha+1)_k}L_k^\alpha(x)=\Gamma(\alpha+1)(tx)^{-\alpha/2}e^tJ_\alpha(2\sqrt{tx}),$$
$$(B47)$$

then

$$p(z,r)=(-1)^{-z/2}e^{-2a(1-R)}J_z[2(1-R)i]$$
$$=e^{-2a(1-R)}I_z[2a(1-R)],\qquad(B48)$$

where $I_z(x)$ is modified Bessel function. Therefore,

$$C(k_\perp,r)=\sum_{z=-\infty}^{\infty}e^{-2a(1-R)}I_z[2a(1-R)]e^{ik_\perp cz},$$
$$(B49)$$

where c is the lattice constant along the z axis. Let $\Phi=k_\perp c$; then

$$C(k_\perp,r)=e^{-2a(1-R)}I_0[2a(1-R)]$$

$$+2e^{-2a(1-R)}\sum_{n=1}^{\infty}I_n[2a(1-R)]\cos(n\Phi),$$
$$(B50)$$

i.e.,

$$C(k_\perp,r)=e^{-2a(1-R)(1-\cos\Phi)}.\qquad(B51)$$

The height-height correlation function is

$$H(r)=\sum_{z=-\infty}^{\infty}z^2e^{-2a(1-R)}I_z[2a(1-R)]=2a(1-R).$$
$$(B52)$$

So

$$C(k_\perp,r)=e^{-H(r)(1-\cos\Phi)}.\qquad(B53)$$

[1] For a review see *Dynamics of Fractal Surfaces*, edited by F. Family and T. Vicsek (World Scientific, Singapore, 1990).

[2] A.-L. Barabási and H. E. Stanley, *Fractal Concepts in Surface Growth* (Cambridge University Press, New York, 1995).

[3] H.-N. Yang, G.-C. Wang, and T.-M. Lu, *Diffraction from Rough Surfaces and Dynamic Growth Fronts* (World Scientific, Singapore, 1993).

[4] S. F. Edwards and D. R. Wilkison, Proc. R. Soc. London Ser. A **381**, 17 (1982).

[5] L. M. Sander, in *Multiple Scattering of Waves in Random Media and Random Rough Surfaces*, edited by V. V. Varadan and V. K. Varadan (Pennsylvania State University Press, University Park, PA, 1985).

[6] F. Family, J. Phys. A **19**, L441 (1986).

[7] R. Jullien and R. Botet, J. Phys. A **18**, 2279 (1985).

[8] J. G. Zabolitzky and D. Stauffer, Phys. Rev. A **34**, 1523 (1986); Phys. Rev. Lett. **57**, 1809 (1986).

[9] J. Kertész and D. E. Wolf, J. Phys. A **21**, 747 (1988); D. E. Wolf and J. Kertész, Europhys. Lett. **4**, 651 (1987).

[10] M. J. Vold, J. Colloid Interface Sci. **14**, 168 (1959).

[11] F. Family and T. Vicsek, J. Phys. A **18**, L75 (1985).

[12] M. Kardar, G. Parisi, and Y.-C. Zhang, Phys. Rev. Lett. **56**, 889 (1986).

[13] J. M. Kim and J. M. Kosterlitz, Phys. Rev. Lett. **62**, 2289 (1989).

[14] S. Das Sarma and P. Tamborrenea, Phys. Rev. Lett. **66**, 325 (1991).

[15] Z.-W. Lai and S. Das Sarma, Phys. Rev. Lett. **66**, 2348 (1991).

[16] L.-H. Tang and T. Nattermann, Phys. Rev. Lett. **66**, 2899 (1991).

[17] Hong Yan, Phys. Rev. Lett. **68**, 3048 (1992).

[18] For a review see Mater. Res. Soc. Bull. **20** (5) (1995).

[19] S. K. Sinha, E. B. Sirota, and S. Garoff, Phys. Rev. B **38**, 2297 (1988).

[20] P.-Z. Wong and A. J. Bray, Phys. Rev. B **37**, 7751 (1988).

[21] See H.-N. Yang, G.-C. Wang, and T.-M. Lu, *Diffraction from Rough Surfaces and Dynamic Growth Fronts* (Ref. 3), Chap. III, pp. 82–135; Phys. Rev. B **47**, 3911 (1993).

[22] See, for example, H.-N. Yang, G.-C. Wang, and T.-M. Lu, Phys. Rev. Lett. **73**, 2348 (1994).

[23] T. Halpin-Healy and Y.-C. Zhang, Phys. Rep. **254**, 215 (1995).

[24] M. C. Bartelt and J. W. Evans, Phys. Rev. Lett. **75**, 4250 (1995); J. W. Evans and M. C. Bartelt, Langmuir **12**, 217 (1996).

[25] J. L. Brown, IRE Trans. **IT-4**, 172 (1958).

[26] E. Masry, Proc. IEEE **57**, 1771 (1969).

[27] P. Beckmann, *Orthogonal Polynomials for Engineers and Physicists* (Golem, Boulder, 1973).

[28] G. Palasantzas, Phys. Rev. E **48**, 14 472 (1993).

[29] Larry C. Andrews, *Special Functions of Mathematics for Engineers*, 2nd ed. (McGraw-Hill, New York, 1992).

[30] Y.-P. Zhao, H.-N. Yang, G.-C. Wang, and T.-M. Lu, Appl. Phys. Lett. **68**, 3063 (1996).

[31] H. Risken, *The Fokker-Planck Equations: Methods of Solution and Applications* (Springer-Verlag, New York, 1984); J. Honerkamp, *Stochastic Dynamical System: Concepts, Numerical Methods, Data Analysis*, translated by K. Lindenberg (VCH, New York, 1994).

[32] G. Szego, *Orthogonal Polynomials*, American Mathematical Society Colloquium Vol. XXIII (American Mathematical Society, Providence, RI, 1959), p. 34.